HYPERSPECTRAL IMAGE CLASSIFICATION OF GRASS SPECIES IN NORTHEAST JAPAN

Sildomar T. Monteiro[*a], *Kuniaki Uto*[b], *Yukio Kosugi*[b], *Kunio Oda*[c], *Yoshiyuki Iino*[d] *and Genya Saito*[d]

[a]Australian Center for Field Robotics
University of Sydney, Australia
[b] Tokyo Institute of Technology, Japan
[c] Yamagata Prefectural College of Agriculture, Japan
[d] Tohoku University, Japan

ABSTRACT

This paper investigates the application of artificial neural networks for classifying grass species from hyperspectral image data. High-resolution spatial and spectral data of localized fields were collected using a hyperspectral sensor mounted on the tip of a crane. The hyperspectral datasets are processed using normalization and second derivative in order to reduce the effect of variations in the intensity level of reflectance and to improve the classification accuracy and generalization performance of the neural network-based model. An experimental comparison of the pre-processing methods shows that the best classification accuracy is obtained by the second derivative transformed dataset. Normalization, and a combination of both methods, did not improve accuracy of the neural network models of our experimental datasets more than simple raw reflectance.

Index Terms— Hyperspectral, image classification, neural networks, normalization, second derivative

1. INTRODUCTION

Spectral signature analysis of hyperspectral image data has been applied mainly for land cover classification [1]. Nevertheless, applications for material identification are still difficult to be realized, especially when targets present high spectral similarity [2]. Conventional land cover classification methods allow easy distinction among different materials, e.g., bare soil, vegetation and minerals, however the identification of different varieties of the same class of material, e.g., identifying grass vegetation species, is still a challenging task. In the case of high-resolution hyperspectral data of localized areas, variations in intensity level of reflectance due to light scattering characteristics of leaves and noise introduced during data acquisition make the classification particularly difficult.

*Thanks to Japan Society for the Promotion of Science (JSPS) for funding. The first author was with the Department of Mechano-Micro Engineering, Interdisciplinary Graduate of School of Science and Engineering, Tokyo Institute of Technology, Japan. Email: s.monteiro@acf.usyd.edu.au.

Japan is an island country composed predominantly of mountains. With limited land and grass, farmers commonly rear animals in barns and feed them forage and grain that are imported. Grass is an important nourishment source for the animals, and rearing and feeding methods have a direct impact on cattle's health and on meat quality. While the development of strong, fast-growing, nutritious grass species is being pursued by agricultural researchers, e.g. [3], the management of grass pastures and land use could benefit from developments in remote sensing sensor technology.

In this paper, we investigate the application of artificial neural network (ANN) models to classify hyperspectral image data of different grass species in northeast Japan. Two data pre-processing methods, normalization and second derivative, were implemented aimed at reducing the effect of variations in reflectance's intensity level and improving the performance of the ANN-based model. A comparison of the pre-processing methods, including a combination of both, is presented.

2. METHODOLOGY

Firstly, the raw data captured by the hyperspectral sensor is converted to reflectance using a "white" standard reference. Then, a three-dimensional low-pass filter is applied to attenuate the dataset's spatial and spectral noise. As an example, the resulting spectral curves of four different grass samples are shown in Fig. 1 (a).

Spatial location of vegetation in the hyperspectral images is identified using the normalized difference vegetation index (NDVI) [4]. Next, the hyperspectral data is transformed using normalization and derivative analysis.

2.1. Normalization

Normalization has been proposed to reduce the effect of variations in absolute reflectance values and highlight the spectral shape information [5].

Assuming that the hyperspectral data can be expressed as

978-1-4244-2808-3/08/$25.00 ©2008 IEEE

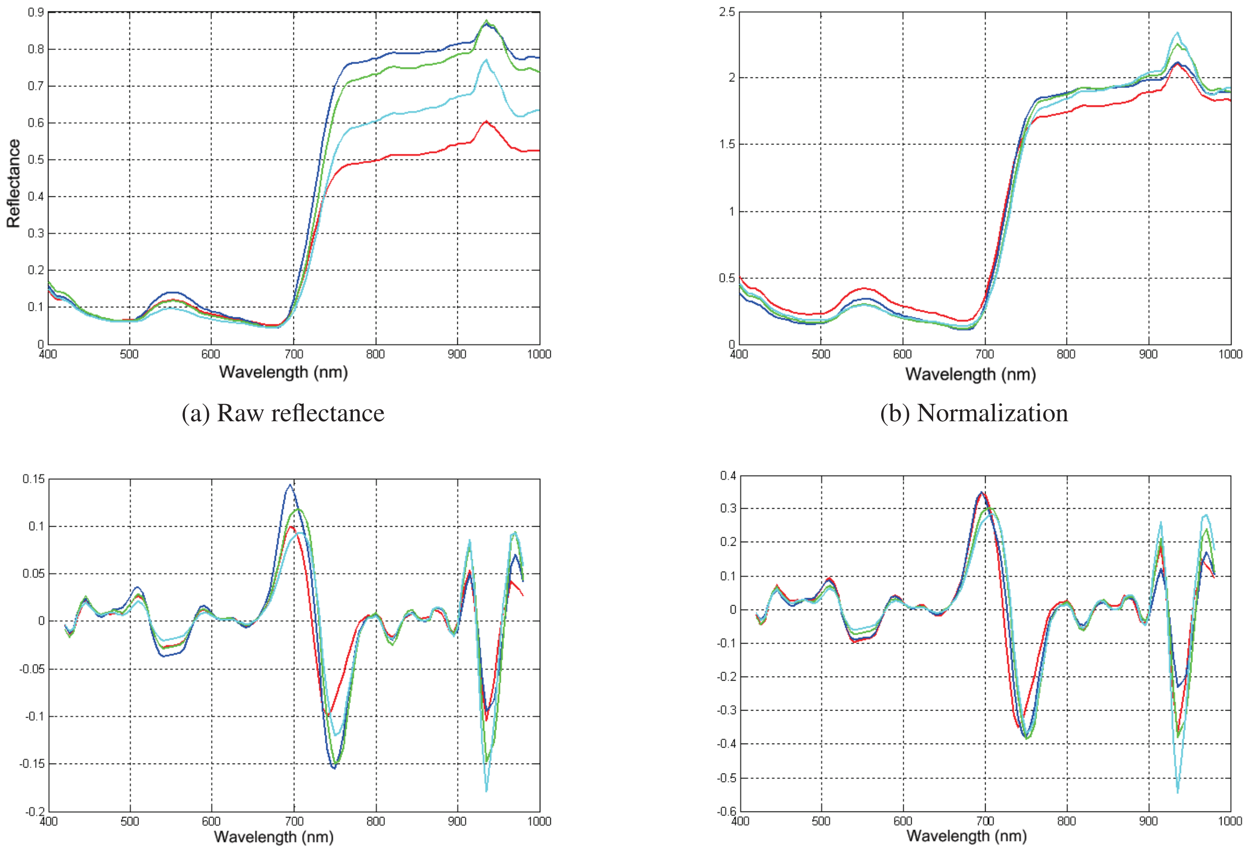

(a) Raw reflectance

(b) Normalization

(c) Second derivative

(d) Normalization and second derivative

Fig. 1. Spectral curves of samples from four different species of grass.

a matrix of reflectance values R, composed of n spectral images $R(\lambda)$, $(\lambda = 1, \ldots, n)$. The normalization equation is defined as

$$\bar{R}(\lambda) = \frac{R(\lambda)}{\mu}, \tag{1}$$

where $\mu = \frac{1}{n}\sum_{\lambda=1}^{n} R(\lambda)$. The normalized spectra of four grass samples are shown in Fig. 1 (b).

2.2. Second Derivative

Derivatives are considered to be theoretically less susceptible to variations in illumination intensity in the remote sensing field. The second derivative has been used in hyperspectral data analysis to increase the estimation accuracy of ANN models [6]. Nevertheless, the derivative process may also accentuate the noise, thus the necessity of using filters to reduce the noise in the datasets.

The derivative of hyperspectral data can be calculated by finite approximation [7]. Given a band resolution $\Delta\lambda$ for the derivatives centered at wavelength λ_v, i.e., a finite separation between adjacent bands, the second derivative is approximated using the following equation

$$\begin{aligned} \left.\frac{d^2R}{d\lambda^2}\right|_v &= \left.\frac{d}{d\lambda}\left(\frac{dR}{d\lambda}\right)\right|_v \\ &\approx \frac{R(\lambda_u) - 2R(\lambda_v) + R(\lambda_w)}{(\Delta\lambda)^2}\,. \end{aligned} \tag{2}$$

Furthermore, this formulation of the second derivative must obey the constraints that $\Delta\lambda = \lambda_w - \lambda_v = \lambda_v - \lambda_u$ and $\lambda_u < \lambda_v < \lambda_w$. The derivation interval was set to 20 nm, which is a reasonable value determined after preliminary experiments. The second derivative transformed spectra of the four grass samples are shown in Fig. 2 (c).

Another dataset is generated by combining both methods, normalization and second derivatives. The raw reflectance data is normalized first, and, after that, the second derivative is applied. This is achieved by replacing $R(\lambda)$ values in Eq. (2) by $\bar{R}(\lambda)$ calculated from Eq. (1). The resulting spectra for the four grass samples are shown in Fig. 1 (d).

Dark pixels and outliers are typically noisy and may affect both the normalization and derivatives. We defined dark

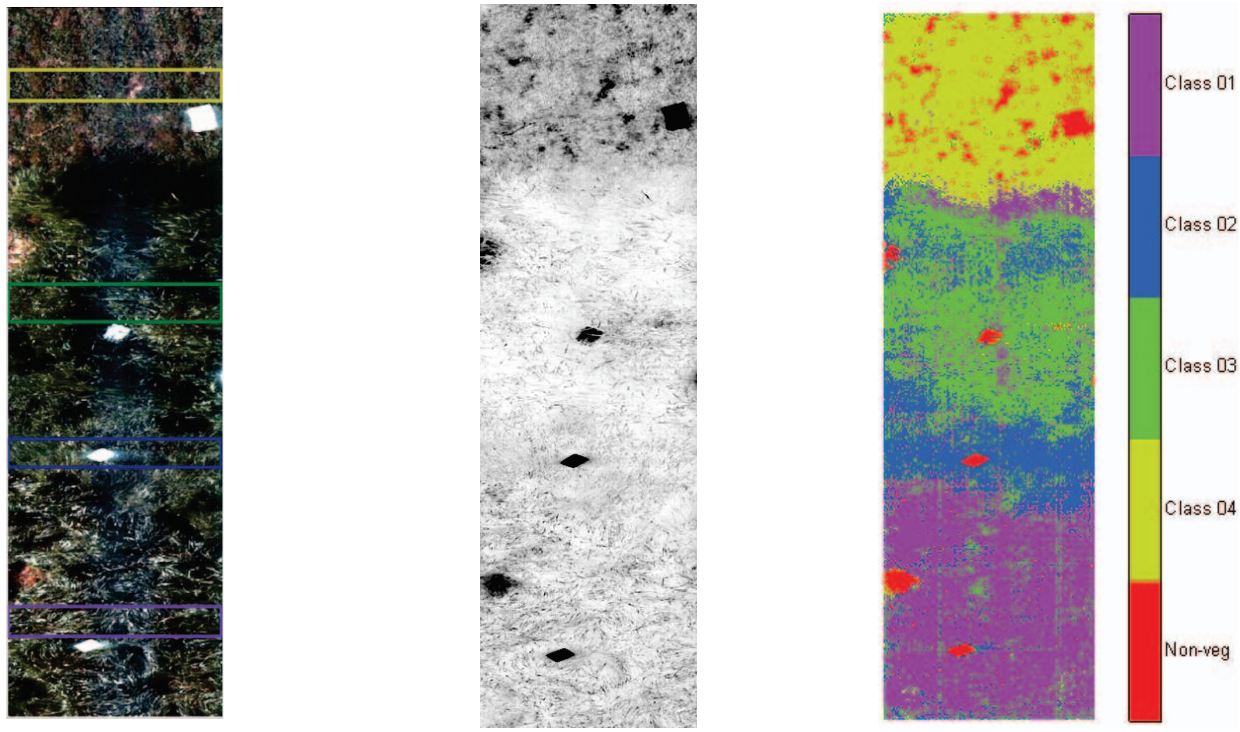

(a) RGB visualization (b) NDVI image (c) ANN classification

Fig. 2. Sample area containing four different grass species, as indicated by the small white labels in (a). The training data for the ANN were randomly taken from selected areas of each grass species, as highlighted by the rectangles in (a).

pixels as spatial points with mean reflectance less than 15% of the maximum possible reflectance. Outliers are calculated from the NDVI value using Chebyshev's inequality. To prevent negative effects on the subsequent ANN training, pixels that fall in either case were excluded from the training data.

2.3. Artificial Neural Network

The ANN implemented is a multilayer perceptron (MLP) network. The proposed architecture is a feed-forward network composed of three layers: one input layer, one hidden layer, and one output layer. The method employed to train the MLP is the scaled conjugate gradient algorithm [8].

The training data is composed of pixels randomly selected from regions where the variety of grass is known. A "mask" is also utilized to mask out undesirable pixels—non-vegetation, as determined by a NDVI threshold, dark pixels and outliers—preventing them from being selected as training data.

The input data is then normalized to fall in the interval $[-1, 1]$. In order to provide better generalization performance, an early stopping method is used. As preparation for the ANN training, the sample dataset is divided into training, validation and test datasets, 50%, 25%, 25%, respectively.

3. EXPERIMENTAL RESULTS

Hyperspectral data was collected using a crane-mounted hyperspectral imaging sensor, which acquires high-resolution spatial and spectral data. Sample data of 11 different grass species were collected during the summer of 2007, around noontime, at Tohoku University's Field Science Center located in Miyagi Prefecture, Japan. The hyperspectral data comprises the visible (400 nm) to the near-infrared (1000 nm) range of the spectrum with pixel resolution of approximately 5 mm per pixel. Figure 2 shows part of the experimental grass field from which samples were taken. An RGB visualization is shown in Fig. 2 (a). Additionally, A visualization of NDVI levels, as gray scale image, is shown in Fig. 2 (b).

The hyperspectral data was processed using a Pentium 4, 3.8 GHz computer with 2 GBytes of RAM. The algorithms were implemented in Matlab. Each MLP network was tested over several independent runs, each starting with random neural network weights. The network presenting the best performance was retained, i.e., model with lower error (mean squared error) and higher classification accuracy (percentage of correctly classified pixels overall). Table 1 shows the numerical results of the best trained ANN, and a summary of the training.

Figure 2 (c) shows an example of the application of the

Table 1. Experimental results—comparison of pre-processing methods for neural network classification.

	Best		Training^c			
Dataset	Accuracy^a	Error^b	Accuracy	Error	Epochs	Time(s)
Raw reflectance	92.66	0.037	90.93 (1.4)	0.045 (0.007)	1026 (40)	403 (106)
Normalized	92.53	0.037	90.39 (2.0)	0.048 (0.01)	837 (172)	338 (104)
2nd Derivate	93.46	0.033	91.43 (3.5)	0.043 (0.018)	523 (54)	190 (50)
Norm. & 2nd Deriv.	91.9	0.041	90.68 (0.99)	0.047 (0.005)	591 (60)	204 (48)

^{c}Values shown are the averages over several runs; standard deviation is shown in parentheses.
^{a}General classification accuracy of the best ANN model.
^{b}Mean squared error.

Table 2. Classification accuracy of the best ANN model, for each class of the sample area shown in Fig. 2 (c).

Class	Accuracy (%)
1	99.66
2	89.58
3	91.68
4	92.92

trained ANN to classify hyperspectral image data. The resulting classification accuracy per class of the best ANN model is shown in Table 2.

4. CONCLUSION

The ANN-based models provided an acceptable accuracy performance to classify hyperspectral image data of the grass samples in our experiments. A comparison of four different datasets—raw reflectance, normalization, second derivative, and normalization followed by second derivative—is presented.

In our experiments, the dataset transformed by second derivative resulted in higher classification accuracy and, in general, normalization did not improve classification performance. Interestingly enough, the combination of the two methods presented the worst performance of all datasets. This may be due to noise introduced by the normalization process that is being amplified by the second derivative, thus offsetting the advantages of the latter.

Normalization is particularly interesting to facilitate human-based assessment of spectral curves of plant samples. On the other hand, the second derivative is less intuitive when used to manually compare spectra. Notwithstanding, the second derivatives generally produce more accurate prediction models based on ANNs. The proposed method permits the application of high-resolution hyperspectral imaging for identifying different grass species in the field without interfering in the growth process.

5. REFERENCES

[1] F. Melgani and L. Bruzzone, "Classification of hyperspectral remote sensing images with support vector machines," *IEEE Trans. Geosci. Remote Sensing*, vol. 42, no. 8, pp. 1778–1790, 2004.

[2] C. Kwan, B. Ayhan, G. Chen, J. Wang, B. Ji, and C.-I Chang, "A novel approach for spectral unmixing, classification, and concentration estimation of chemical and biological agents," *IEEE Trans. Geosci. Remote Sensing*, vol. 44, no. 2, pp. 409–419, 2006.

[3] M. Yayota, M. Kobayashi, and S. Ohtani, "A comparison of nutrient intake and digestibility in beef cows grazed on Nezasa dwarf bamboo (*Pleioblastus chino var. viridis*)-dominated pasture and improved grass pasture.," *Grassland Science*, vol. 49, no. 5, pp. 430–437, 2003.

[4] J.A. Richards and X. Jia, *Remote Sensing Digital Image Analysis, An Introduction*, Springer-Verlag, New York, 4th edition, 2005.

[5] C. Wu, "Normalized spectral mixture analysis for monitoring urban composition using ETM+ imagery," *Remote Sensing of Environment*, vol. 93, no. 4, pp. 480–492, 2004.

[6] S.T. Monteiro, Y. Minekawa, Y. Kosugi, T. Akazawa, and K. Oda, "Prediction of sweetness and amino acid content in soybean crops from hyperspectral imagery," *ISPRS J. Photogrammetry and Remote Sensing*, vol. 62, no. 1, pp. 2–12, 2007.

[7] F. Tsai and W. Philpot, "Derivative analysis of hyperspectral data," *Remote Sensing of Environment*, vol. 66, pp. 41–51, 1998.

[8] M.F. Møller, "A scaled conjugate gradient algorithm for fast supervised learning," *Neural Networks*, vol. 6, pp. 525–533, 1993.